Josephson effect of the superconducting quantum point contact

Akira Furusaki
Department of Applied Physics, University of Tokyo, Bunkyo-ku, Tokyo 113, Japan

Hideaki Takayanagi
Nippon Telegraph and Telephone Corporation Basic Research Laboratories, Musashino-shi, Tokyo 180, Japan

Masaru Tsukada
Department of Physics, University of Tokyo, Bunkyo-ku, Tokyo 113, Japan
(Received 27 September 1991; revised manuscript received 11 December 1991)

The dc Josephson effect of a constriction in a two-dimensional superconductor-semiconductor-superconductor junction, i.e., a superconducting quantum point contact, is investigated theoretically for both long and short constriction lengths compared with the superconducting coherence length. It is shown that the critical current of a ballistic superconducting quantum point contact increases stepwise as a function of its width under appropriate conditions. The step height generally depends on both the superconducting energy gap and junction parameters. The effect of normal reflections at the superconductor-semiconductor interface is also examined.

I. INTRODUCTION

It has recently become possible to study high-mobility devices in which the electrons can travel ballistically, and it is now established that the conductance G of a quantum point contact (QPC) in a two-dimensional electron gas (2DEG) is quantized in units of $e^2/\pi\hbar$.[1-3] This surprising phenomenon results from the quantization of the transverse momentum of the electrons in a constriction having a width of the order of the Fermi wavelength.

One possible extension of these studies on the quantum transport in a 2DEG is to explore the quantum transport of Cooper pairs, i.e., the Josephson effect between two superconductors coupled by a 2DEG in a semiconductor. In fact, the Josephson current through a 2DEG was observed in a Nb/p-InAs/Nb junction before the discovery of the quantized conductance, using the native inversion layer of p-type InAs.[4] However, this junction was a dirty system, where the motion of quasiparticles was not ballistic but diffusive. To our knowledge, a very clean and high-mobility S-Sm-S junction (S and Sm denote superconductor and semiconductor, respectively) has not yet been made, but in the near future, progress in microfabrication and crystal growth technology will make it possible to fabricate high-mobility S-Sm-S Josephson junctions.

Consider a constriction in a 2DEG of a high-mobility S-Sm-S junction with gate electrodes. The constriction acts as a superconducting quantum point contact (SQPC) of variable width, whose normal-state conductance is quantized. It is well known that the critical (maximum) supercurrent I_C of a classical Josephson point contact is given by $\pi G\Delta_0/e$,[5] where Δ_0 is the order parameter of the superconductor. Thus, it is very likely that I_C of the S-Sm-S junction is quantized in units of $e\Delta_0/\hbar$, if the resistance of the S-Sm interface is much smaller than the quantized resistance of the SQPC. However, this scenario is too simple since the scale of two characteristic lengths is neglected.[6] The first one is the Fermi wavelength λ_F, which determines whether the wave nature of electrons appears in the transport through the constriction. The other one is the coherence length $\xi = \hbar v_F/\pi\Delta_0$, where v_F is the Fermi velocity of the semiconductor, not the superconductor. It is known that the Josephson current flows mainly via bound states (excitation energy $E < \Delta_0$), and the number of bound states is roughly proportional to L/ξ, where L is the length of the semiconductor. For very short junctions ($L \ll \xi$) the current is carried by a single bound state while many bound states contribute to the Josephson current for very long junctions ($L \gg \xi$). It is the coherence length ξ that determines the nature of the supercurrent flow. The critical current is quantized in units of $e\Delta_0/\hbar$ only for S-Sm-S junctions whose semiconductor length is much shorter than the coherence length,[7] as will be discussed in Sec. III.

The Josephson effect through a small number of channels, i.e., the resonant tunneling in a quantum box coupled with two superconductors, has very recently been studied by van Houten.[8] He also briefly mentioned a possible combination of ballistic devices and superconductors. The issue of the critical-current quantization for an SQPC has been studied by Furusaki *et al.*,[9] and the special case of a very short constriction has been investigated by Beenakker and van Houten.[7,10] An SQPC coupled to another electron reservoir has also been considered by van Wees *et al.*[11]

This paper gives a more detailed description of the dc Josephson effect of SQPC's than previous papers.[9,12] The theory of Beenakker and van Houten[7,10] is included in

our theory as a special case of a very short point contact. We demonstrate that the critical current shows a stepwise increase as the constriction becomes wider. Each time a new channel opens in the constriction, the critical current increases abruptly. The step height of the critical current in general depends on junction parameters, such as the separation L between two superconductors, as well as on the superconducting energy gap Δ_0. On the other hand, when the normal reflection (electron→electron or hole→hole) at S-Sm interfaces dominates, the critical current shows peaks due to resonant tunneling instead of the stepwise increase.

Section II describes the calculation method for the dc Josephson current using a simple two-dimensional model. Section III investigates the case where the width of the constriction varies slowly compared with the Fermi wavelength. In this case the scattering between the channels is negligible, and hence we can calculate the dc Josephson current analytically in a simplified WKB approximation. Section IV examines the opposite limit where the width changes suddenly and the scattering between the channels is no longer negligible. The method of numerical calculation is explained in detail and the results for a simple rectangular model are given. The effect of normal reflections at the S-Sm interfaces on the Josephson effect is studied in Sec. V. The main results are summarized in Sec. VI.

II. METHOD OF CALCULATION

In this section, the dc Josephson current is calculated using the temperature Green's function which is constructed from the eigenfunctions of the Bogoliubov-de Gennes (BdG) equation.[13] It is shown that the Josephson current is given by the scattering amplitude of Andreev reflection.[14,15]

We treat an SQPC as a two-dimensional system, and take the x axis along the constriction; the net Josephson current flows in the x direction. It is assumed that the transport of quasiparticles with an effective mass m is ballistic and that no magnetic field is applied. The motion of the quasiparticles is governed by the BdG equation

$$\begin{pmatrix} H(x,y) & \Delta(x,y) \\ \Delta^*(x,y) & -H(x,y) \end{pmatrix} \begin{pmatrix} u(x,y) \\ v(x,y) \end{pmatrix} = E \begin{pmatrix} u(x,y) \\ v(x,y) \end{pmatrix}, \tag{2.1}$$

where $H(x,y)$ is the single-electron Hamiltonian,

$$H(x,y) = -\frac{\hbar^2}{2m}\left(\frac{\partial^2}{\partial x^2} + \frac{\partial^2}{\partial y^2}\right) + U(x,y) - E_F \tag{2.2}$$

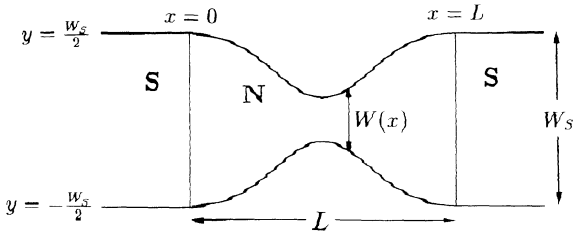

FIG. 1. Schematic drawing of a two-dimensional model for an SQPC.

and $\Delta(x,y)$ is the pair potential. The width of the system in the y direction is assumed to vary only in the semiconductor ($0 < x < L$) and to be constant W_S in the superconductor ($x < 0$ and $x > L$). The geometry of the system is defined by the hard-wall boundary condition (Fig. 1). That is, the wave functions vanish at the boundary.

The Fermi momentum of the semiconductor is generally different from that of the superconductor. Thus the potential $U(x,y)$ has different values in each material. This difference causes normal reflections at the S-Sm interfaces, which reduces both the Cooper-pair amplitude penetrating into the semiconductor and the Josephson current.[16,17] We assume that $U(x,y)$ is constant in the superconducting region.

In principle the pair potential should be determined from the self-consistent gap equation, but instead we simply assume that it is constant in the superconducting region and vanishes in the normal region:

$$\begin{aligned}\Delta(x,y) &= \Delta(x) \\ &= \Delta_0\left[\Theta(-x) + \exp(i\varphi)\Theta(x-L)\right].\end{aligned} \tag{2.3}$$

In many cases this rectangular pair potential is sufficient for obtaining quantitatively correct results and has been adopted by a number of authors.[18–25] In particular, Plehn *et al.* have shown that the spatial variation of the pair potential near the interfaces can be simulated by using an effective S-S separation L^* with a rectangular pair potential.[25]

The solution of Eq. (2.2) is a linear combination of plane waves in the regions $x < 0$ and $x > L$. The wave function representing the process in which an electron-like quasiparticle is injected from the left-hand side is written as

$$\psi_{1j}(x,y) = e^{ip_j^+ x}\sqrt{\frac{2}{W_S}}\sin\left[q_j\left(y+\frac{W_S}{2}\right)\right]\begin{pmatrix} u_0 \\ v_0 \end{pmatrix} + \sqrt{\frac{2}{W_S}}\sum_{k=1}^{\infty}\left[a_{1jk}e^{ip_k^- x}\begin{pmatrix} v_0 \\ u_0 \end{pmatrix} + b_{1jk}e^{-ip_k^+ x}\begin{pmatrix} u_0 \\ v_0 \end{pmatrix}\right]\sin\left[q_k\left(y+\frac{W_S}{2}\right)\right], \tag{2.4}$$

if $x < 0$, and

$$\psi_{1j}(x,y) = \sqrt{\frac{2}{W_S}} \sum_{k=1}^{\infty} \left[c_{1jk} e^{ip_k^+ x} \begin{pmatrix} u_0 e^{i\varphi/2} \\ v_0 e^{-i\varphi/2} \end{pmatrix} + d_{1jk} e^{-ip_k^- x} \begin{pmatrix} v_0 e^{i\varphi/2} \\ u_0 e^{-i\varphi/2} \end{pmatrix} \right] \sin\left[q_k \left(y + \frac{W_S}{2} \right) \right], \tag{2.5}$$

if $x > L$, where j is a positive integer,

$$p_k^{\pm} = \sqrt{\frac{2m}{\hbar^2}(E_F \pm \Omega) - q_k^2}, \quad q_k = \frac{k\pi}{W_S}, \quad u_0 = \sqrt{\frac{1}{2}\left(1 + \frac{\Omega}{E}\right)}, \quad v_0 = \sqrt{\frac{1}{2}\left(1 - \frac{\Omega}{E}\right)}, \tag{2.6}$$

and $\Omega = \sqrt{E^2 - \Delta_0^2}$.

The coefficients a_{1jk}, b_{1jk}, c_{1jk}, and d_{1jk} are functions of the energy E and the phase difference φ across two superconductors, and they are determined by the matching conditions discussed in the following sections. The retarded Green's function is obtained by combining the above wave function and three other types of wave functions. The method is briefly described in the Appendix.

The dc Josephson current I can be calculated from the temperature Green's function, $G_{\omega_n}(x,y:x',y')$, which is obtained by analytic continuation, $E + i0^+ \to i\omega_n$, from the retarded Green's function. Here ω_n is the Matsubara frequency, $\pi(2n+1)/\beta$ ($n = 0, \pm 1, \pm 2, \ldots$), at temperature $T = 1/k_B\beta$. Taking into account the charge-conservation law, the current at $x = 0$ is calculated:

$$\begin{aligned} I &= \frac{e\hbar}{2im} \int_{-W_S/2}^{W_S/2} dy \left(\frac{\partial}{\partial x'} - \frac{\partial}{\partial x} \right) \frac{1}{\beta} \sum_{\omega_n} \mathrm{Tr}[G_{\omega_n}(x,y:x',y')] \Big|_{x=x'=0, y=y'} \\ &= \frac{e\Delta_0}{2\hbar\beta} \sum_{\omega_n} \frac{1}{\Omega_n} \sum_{j=1}^{\infty} (p_j^+ + p_j^-) \left(\frac{a_{1jj}(\varphi, i\omega_n)}{p_j^+} - \frac{a_{2jj}(\varphi, i\omega_n)}{p_j^-} \right), \end{aligned} \tag{2.7}$$

where $\Omega_n = (\omega_n^2 + \Delta_0^2)^{1/2}$. If the kinetic energy of the jth channel along the x axis is much larger than the energy gap, that is, if $p_j^+ \approx p_j^- \approx p_j \equiv (2mE_F/\hbar^2 - q_j^2)^{1/2}$, Eq. (2.7) can be written as

$$I \approx \frac{e\Delta_0}{\hbar\beta} \sum_{\omega_n} \frac{1}{\Omega_n} \sum_{j=1}^{N} [a_{1jj}(\varphi, i\omega_n) - a_{1jj}(-\varphi, i\omega_n)], \tag{2.8}$$

where N is the largest integer to make p_j a real number, i.e., the number of open channels. Thus the Josephson current is given by the Andreev-scattering amplitude a_{1jj}.

The comment on Eq. (2.7) is here in order. So far we have derived the expression of the dc Josephson current in terms of imaginary energy $i\omega_n$: $I = \frac{1}{\beta} \sum_{\omega_n} I(i\omega_n)$. This expression can be rewritten in terms of real energy E as

$$I = \frac{1}{\beta} \sum_{\omega_n} I(i\omega_n) = \int_{C_1+C_2} \frac{dz}{4\pi i} I(z) \tanh\frac{\beta z}{2} = \frac{1}{\pi} \int_{\Delta_0}^{\infty} dE\, \mathrm{Im}[I(E)] \tanh\frac{\beta E}{2} + \int_C \frac{dE}{4\pi i} I(E) \tanh\frac{\beta E}{2}. \tag{2.9}$$

The contours C_1, C_2, and C are depicted in Fig. 2. The first term of the right-hand side of Eq. (2.9) is the contribution from continuous energy levels with $E > \Delta_0$. Since the scattering amplitude of the Andreev reflection has a pole at $E = \pm E_B$, where E_B is a bound state's energy ($0 < E_B < \Delta_0$), the second term gives the contribution from bound states (discrete levels). Thus, our formula (2.7) contains both contributions in a single expression. We also note that Eq. (2.9) should coincide with a result obtained from the relation between the Josephson current and φ dependence of excitation spectra.[10]

III. ADIABATIC TRANSPORT

In this section we consider the case where the width of the constriction $W(x)$ varies slowly compared with the Fermi wavelength. In this case the scattering between the channels can be neglected so that the Andreev-scattering amplitude a_{ijk} is nonzero only for $j = k$.

We solve the BdG equation in the WKB approximation[26] to obtain the amplitude a_{ij} ($= a_{ijj}$). In this and the next section we put $U(x,y) = 0$ to concentrate on the quantum conduction of the supercurrent through the constriction by restricting our discussion to the case of an ideal S-Sm contact. The effect of normal reflections will be discussed in Sec. V. From the assumption of the adiabatic transport, the wave function of the quasiparticles in the jth channel can be written as

$$\psi_j(x,y) = \sqrt{\frac{2}{W(x)}}\phi_j(x)\sin\left[j\pi\left(\frac{y}{W(x)}+\frac{1}{2}\right)\right], \tag{3.1}$$

where a two-component wave function $\phi_j(x)$ obeys a modified BdG equation:

$$\begin{pmatrix} -\frac{\hbar^2}{2m}\left[\frac{d^2}{dx^2}-\left(\frac{j\pi}{W(x)}\right)^2\right]-E_F & \Delta(x) \\ \Delta^*(x) & \frac{\hbar^2}{2m}\left[\frac{d^2}{dx^2}-\left(\frac{j\pi}{W(x)}\right)^2\right]+E_F \end{pmatrix}\phi_j(x) = E\phi_j(x). \tag{3.2}$$

We solve Eq. (3.2), assuming the form of the wave function as

$$\phi_j(x) = \begin{cases} e^{ip_j^+x}\begin{pmatrix}u_0\\v_0\end{pmatrix} + a_{1j}e^{ip_j^-x}\begin{pmatrix}v_0\\u_0\end{pmatrix} + b_{1j}e^{-ip_j^+x}\begin{pmatrix}u_0\\v_0\end{pmatrix}, & x<0 \\ \left(\alpha_{1j}e^{ik_j^+(x)x}+\beta_{1j}e^{-ik_j^+(x)x}\right)\begin{pmatrix}1\\0\end{pmatrix} + \left(\gamma_{1j}e^{ik_j^-(x)x}+\delta_{1j}e^{-ik_j^-(x)x}\right)\begin{pmatrix}0\\1\end{pmatrix}, & 0<x<L \\ c_{1j}e^{ip_j^+x}\begin{pmatrix}u_0e^{i\varphi/2}\\v_0e^{-i\varphi/2}\end{pmatrix} + d_{1j}e^{-ip_j^-x}\begin{pmatrix}v_0e^{i\varphi/2}\\u_0e^{-i\varphi/2}\end{pmatrix}, & x>L, \end{cases} \tag{3.3}$$

where

$$k_j^{\pm}(x) = \left[\frac{2m}{\hbar^2}(E_F\pm E)-\left(\frac{j\pi}{W(x)}\right)^2\right]^{1/2}. \tag{3.4}$$

The matching conditions at $x=0$ and L are given, within the Andreev and WKB approximation, by

$$\begin{aligned} &u_0+a_{1j}v_0=\alpha_{1j},\quad \alpha_{1j}\exp\left(i\int_0^L k_j^+(x)dx\right) = c_{1j}u_0\exp\left[i\left(p_j^+L+\frac{i}{2}\varphi\right)\right], \\ &v_0+a_{1j}u_0=\gamma_{1j},\quad \gamma_{1j}\exp\left(i\int_0^L k_j^-(x)dx\right) = c_{1j}v_0\exp\left[i\left(p_j^+L-\frac{i}{2}\varphi\right)\right], \\ &b_{1j}=d_{1j}=\beta_{1j}=\delta_{1j}=0. \end{aligned} \tag{3.5}$$

The solution of Eq. (3.5) is

$$a_{1j}(\varphi,E) = \frac{\Delta_0[\exp(i\Phi_j)-\exp(i\varphi)]}{(E+\Omega)\exp(i\varphi)-(E-\Omega)\exp(i\Phi_j)}, \tag{3.6}$$

where $\Phi_j=\int_0^L[k_j^+(x)-k_j^-(x)]dx$, and hence the dc Josephson current is obtained from Eqs. (2.8) and (3.6) as

$$I = \frac{2e\Delta_0^2}{\hbar\beta}\sum_{j=1}^{N}\sum_{\omega_n}\frac{\sin\varphi}{(2\omega_n^2+\Delta_0^2)\cosh\tilde{\Phi}_j+2\omega_n\Omega_n\sinh\tilde{\Phi}_j+\Delta_0^2\cos\varphi}, \tag{3.7}$$

where $\tilde{\Phi}_j=-i\Phi_j(E\to i\omega_n)$.

To see the qualitative feature of this result, we shall consider two interesting limits. First, in the limit $L\ll\xi$, Eq. (3.7) becomes

$$I = N\frac{2e\Delta_0^2}{\hbar\beta}\sum_{\omega_n}\frac{\sin\varphi}{2\omega_n^2+\Delta_0^2+\Delta_0^2\cos\varphi} = N\frac{e\Delta_0}{\hbar}\sin(\varphi/2)\tanh\left(\frac{\Delta_0}{2k_BT}\cos(\varphi/2)\right), \tag{3.8}$$

which is a natural extension of the Kulik and Omel'yanchuk's result for a classical superconducting point contact,[5] and is in accordance with Eq. (17) of Ref. 7. The Josephson current is a multiple of the supercurrent carried by a single channel which depends only on Δ_0 except for universal quantities e and $\hbar$ at zero temperature. Thus, the critical current I_C will increase stepwise as the constriction becomes wider, and the step height is $e\Delta_0/\hbar$ at zero temperature.

On the other hand, if $L\gg\xi$, Eq. (3.7) can be written at zero temperature as[20,27]

$$I = \frac{4e}{\pi\hbar}\sum_j\sum_{n=0}^{\infty}\sin(n\varphi)\int_0^{\infty}dE\left(\frac{E-\Omega}{E+\Omega}\right)^n\exp\left(-\frac{2nEL}{\hbar v_j}\right) \approx \frac{e}{\pi L}\sum_{j=1}^{N}v_j\varphi \qquad (-\pi<\varphi<\pi). \tag{3.9}$$

Here we have introduced a velocity v_j defined by

$$v_j = \left(\frac{1}{L} \int_0^L dx \frac{m}{\hbar k_j^0(x)} \right)^{-1}, \tag{3.10}$$

with $k_j^0(x) = \{2mE_F/\hbar^2 - [j\pi/W(x)]^2\}^{1/2}$, and we have substituted $2EL/\hbar v_j$ for $\Phi_j(E)$. Recalling that the critical current of a long S-N-S weak link is proportional to ev_F/L,[20–22] where v_F is the Fermi velocity, Eq. (3.9) can be easily understood. I_C depends on junction parameters such as L and v_j which is a kind of spatial average of velocity, and does not always show a clear stepwise change. Even when it increases stepwise, each step height may not be the same, which contrasts well with the universality of the step height in the limit $L \ll \xi$ mentioned above[7] as well as with that of the conductance quantization.[1,2]

Let us first examine the simplest case of $W(x) = W_0$ (const). In this case the assumption of the adiabatic transport holds exactly, and the quantization of the normal-state conductance is exact.[1] Conversely, Eq. (3.9) implies that the critical current does not show a clear stepwise increase as a function of the width for $L \gg \xi$ since the spatial average of velocity v_j will increase rather smoothly. Figure 3 shows the critical current at zero temperature calculated from Eq. (3.7) as a function of W_0. Here we set the carrier density $N = 5 \times 10^{11}$ cm^{-2}, $\Delta_0(T = 0\ \text{K}) = 1$ meV, and $m = 0.024m_e$ with m_e being the electronic mass.[28] These values of the parameters will be used again in the following numerical calculations.

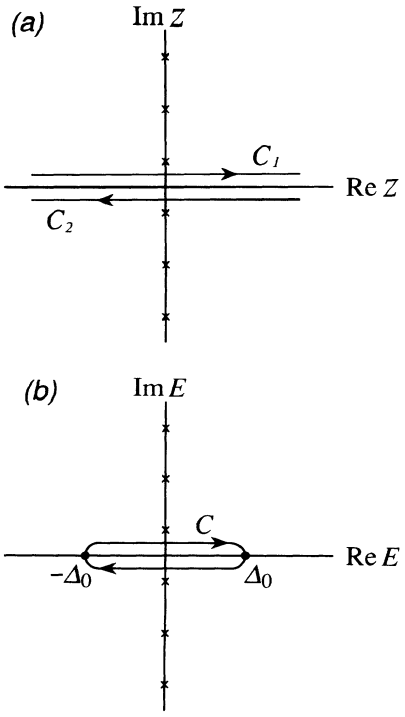

FIG. 2. The contours in Eq. (2.9): (a) C_1 and C_2 and (b) C.

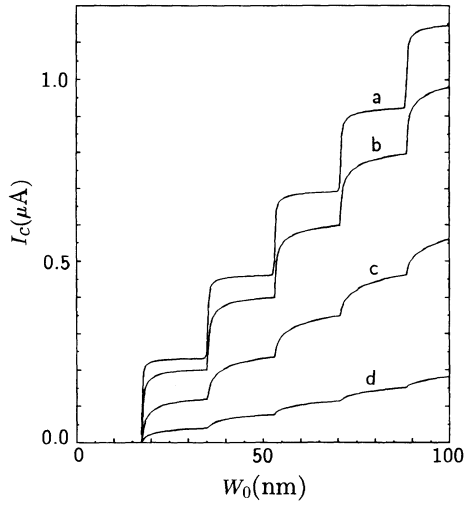

FIG. 3. The critical current in a junction of constant width as a function of the width at zero temperature: (a) $L = 25$ nm, (b) $L = 100$ nm, (c) $L = 500$ nm, and (d) $L = 2500$ nm.

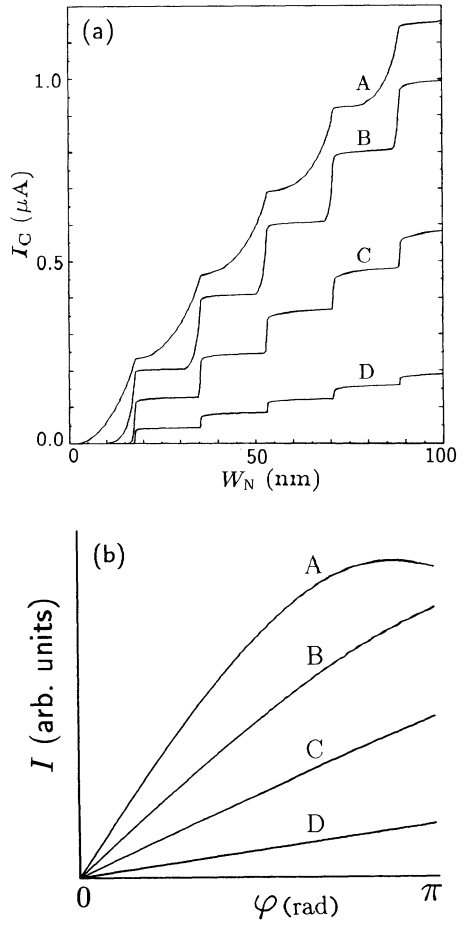

FIG. 4. (a) The critical current vs the minimum width and (b) the Josephson current vs the phase difference. $L =$ 25 nm (A), 100 nm (B), 500 nm (C), and 2500 nm (D).

With this carrier density, an 18-nm increase in W_0 corresponds to the opening of another channel. The coherence length $\xi = \hbar v_F/\pi\Delta_0$ is 180 nm. One can notice that the behavior of I_C is completely different for the two limits, $L \gg \xi$ and $L \ll \xi$. As expected, I_C shows a nearly linear increase in the case of $L \gg \xi$, while I_C increases stepwise in the opposite limit.

Next we shall examine an ordinary SQPC whose width varies spatially (Fig. 1). To be specific, we assume that the width $W(x)$ varies as

$$W(x) = \frac{1}{1-e^{-4}}\left\{ W_S - W_N e^{-4} - (W_S - W_N)\exp\left[-16\left(\frac{x}{L} - \frac{1}{2}\right)^2\right]\right\}. \tag{3.11}$$

Figure 4(a) shows the critical current as a function of the minimum width W_N for a fixed value of $W_S = 120$ nm. The dc Josephson current as a function of the phase difference is also shown in Fig. 4(b). The curves correspond to the cases of $L < \xi$ (A), $L \approx \xi$ (B), and $L > \xi$ (C and D). In Fig. 4(a), I_C increases stepwise for the two cases of longer L while in the upper curve the contribution from the tunnel current through the closed channels smears the steps. It is interesting to note that the step height of each curve is strongly dependent on the length L and is less than $e\Delta_0/\hbar = 0.24\,\mu$A. Moreover the step height of the lower curve decreases as the critical current increases. The change in the current-phase ($I - \varphi$) relation from $I \propto \sin(\varphi/2)$ for short SQPC's to $I \propto \varphi$ for long SQPC's is clearly seen in Fig. 4(b). The difference between the results for $L \gg \xi$ shown in Figs. 3 and 4(a) suggests that spatial variation of the constriction width is necessary to observe a clear stepwise increase in the critical current. The geometry of the system is one of the important factors to determine the supercurrent flow in SQPC's. Another example of the geometrical effect, geometrical resonance, is discussed in the next section.

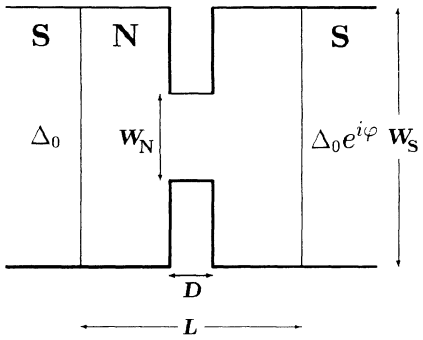

FIG. 5. Schematic drawing of the model with a rectangular constriction.

IV. NONADIABATIC TRANSPORT

In this section we examine the case where the width of an SQPC changes suddenly in the normal region. The geometry of the system is shown in Fig. 5; the width is assumed to be W_S for $x < x_-(= (L - D)/2)$ and for $x > x_+(= (L + D)/2)$, and to be W_N for $x_- < x < x_+$. It is not a trivial issue whether the critical current increases stepwise as a function of the width W_N in such a situation that the mode conversion, i.e., the scattering between the channels at $x = x_+$ and x_-, is important. The dc Josephson current is calculated by a fully numerical method as described below.

In this system the wave function $\psi_{1j}(x, y)$ can be written as

$$\psi_{1j}(x,y) = \begin{cases}
e^{ip_j^+ x}\sin\left[q_j\left(y+\frac{W_S}{2}\right)\right]\begin{pmatrix}u_0\\ v_0\end{pmatrix} \\
\quad +\sum_{l=1}^{\infty}\left[a_{1jl}e^{ip_l^- x}\begin{pmatrix}v_0\\ u_0\end{pmatrix} + b_{1jl}e^{-ip_l^+ x}\begin{pmatrix}u_0\\ v_0\end{pmatrix}\right]\sin\left[q_l\left(y+\frac{W_S}{2}\right)\right], & x < 0 \\
\sum_{l=1}^{\infty}\left[\left(\alpha_{1jl}^{(1)}e^{ik_l^+ x} + \beta_{1jl}^{(1)}e^{-ik_l^+(x-x_-)}\right)\begin{pmatrix}1\\ 0\end{pmatrix}\right. \\
\quad \left. + \left(\gamma_{1jl}^{(1)}e^{ik_l^-(x-x_-)} + \delta_{1jl}^{(1)}e^{-ik_l^- x}\right)\begin{pmatrix}0\\ 1\end{pmatrix}\right]\sin\left[q_l\left(y+\frac{W_S}{2}\right)\right], & 0 < x < x_- \\
\sum_{l=1}^{\infty}\left[\left(\alpha_{1jl}^{(2)}e^{i\tilde{k}_l^+(x-x_-)} + \beta_{1jl}^{(2)}e^{-i\tilde{k}_l^+(x-x_+)}\right)\begin{pmatrix}1\\ 0\end{pmatrix}\right. \\
\quad \left. + \left(\gamma_{1jl}^{(2)}e^{i\tilde{k}_l^-(x-x_+)} + \delta_{1jl}^{(2)}e^{-i\tilde{k}_l^-(x-x_-)}\right)\begin{pmatrix}0\\ 1\end{pmatrix}\right]\sin\left[\tilde{q}_l\left(y+\frac{W_N}{2}\right)\right], & x_- < x < x_+ \\
\sum_{l=1}^{\infty}\left[\left(\alpha_{1jl}^{(3)}e^{ik_l^+(x-x_+)} + \beta_{1jl}^{(3)}e^{-ik_l^+(x-L)}\right)\begin{pmatrix}1\\ 0\end{pmatrix}\right. \\
\quad \left. + \left(\gamma_{1jl}^{(3)}e^{ik_l^-(x-L)} + \delta_{1jl}^{(3)}e^{-ik_l^-(x-x_+)}\right)\begin{pmatrix}0\\ 1\end{pmatrix}\right]\sin\left[q_l\left(y+\frac{W_S}{2}\right)\right], & x_+ < x < L \\
\sum_{l=1}^{\infty}\left[c_{1jl}e^{ip_l^+(x-L)}\begin{pmatrix}u_0e^{i\varphi/2}\\ v_0e^{-i\varphi/2}\end{pmatrix} + d_{1jl}e^{-ip_l^-(x-L)}\begin{pmatrix}v_0e^{i\varphi/2}\\ u_0e^{-i\varphi/2}\end{pmatrix}\right]\sin\left[q_l\left(y+\frac{W_S}{2}\right)\right], & x > L,
\end{cases} \tag{4.1}$$

where

$$k_l^{\pm}=\sqrt{\frac{2m}{\hbar^2}(E_F\pm E)-q_l^2}\,,\quad \tilde{k}_l^{\pm}=\sqrt{\frac{2m}{\hbar^2}(E_F\pm E)-\tilde{q}_l^2}\,,\quad q_l=\frac{l\pi}{W_S},\quad \tilde{q}_l=\frac{l\pi}{W_N}. \tag{4.2}$$

In practical calculations, the number of modes must be cut off to be finite (M_N for $x_- < x < x_+$ and M_S for $x < x_-$ and $x > x_+$), and we set $M_N \geq 20$ and $M_S \geq 40$ in numerical calculations.

The matching equations at $x = 0$, x_-, x_+, and L are transformed into two sets of equations in the Andreev approximation. The first set consists of $4 \times M_S$ equations:

$$\begin{aligned}
&\frac{2}{W_S}\sum_m S_{lm}\left(\alpha_{1jm}^{(2)}+\beta_{1jm}^{(2)}e^{i\tilde{k}_m^+D}\right)=(u_0\delta_{jl}+a_{1jl}v_0)e^{ik_l^+x_-}+b_{1jl}u_0e^{-ik_l^+x_-},\\
&\frac{2}{W_S}\sum_m S_{lm}\left(\gamma_{1jm}^{(2)}e^{-i\tilde{k}_m^-D}+\delta_{1jm}^{(2)}\right)=(v_0\delta_{jl}+a_{1jl}u_0)e^{ik_l^-x_-}+b_{1jl}v_0e^{-ik_l^-x_-},\\
&\frac{2}{W_S}\sum_m S_{lm}\left(\alpha_{1jm}^{(2)}e^{i\tilde{k}_m^+D}+\beta_{1jm}^{(2)}\right)=e^{i\varphi/2}\left(c_{1jl}u_0e^{-ik_l^+x_-}+d_{1jl}v_0e^{ik_l^+x_-}\right),\\
&\frac{2}{W_S}\sum_m S_{lm}\left(\gamma_{1jm}^{(2)}+\delta_{1jm}^{(2)}e^{-i\tilde{k}_m^-D}\right)=e^{-i\varphi/2}\left(c_{1jl}v_0e^{-ik_l^-x_-}+d_{1jl}u_0e^{ik_l^-x_-}\right),
\end{aligned} \tag{4.3}$$

where

$$S_{lm}=\int_{-W_N/2}^{W_N/2}\sin\left[q_l\left(y+\frac{W_S}{2}\right)\right]\sin\left[\tilde{q}_m\left(y+\frac{W_N}{2}\right)\right]dy. \tag{4.4}$$

The other set of $4 \times M_N$ equations comes from the matching of the derivative of the wave function and is given by

$$\begin{aligned}
&\tilde{k}_m^0\left(\alpha_{1jm}^{(2)}-\beta_{1jm}^{(2)}e^{i\tilde{k}_m^+D}\right)=\frac{2k_j^0}{W_N}S_{jm}u_0e^{ik_j^+x_-}+\frac{2}{W_N}\sum_l k_l^0S_{lm}\left(a_{1jl}v_0e^{ik_l^+x_-}-b_{1jl}u_0e^{-ik_l^+x_-}\right),\\
&\tilde{k}_m^0\left(\gamma_{1jm}^{(2)}e^{-i\tilde{k}_m^-D}-\delta_{1jm}^{(2)}\right)=\frac{2k_j^0}{W_N}S_{jm}v_0e^{ik_j^-x_-}+\frac{2}{W_N}\sum_l k_l^0S_{lm}\left(a_{1jl}u_0e^{ik_l^-x_-}-b_{1jl}v_0e^{-ik_l^-x_-}\right),\\
&\tilde{k}_m^0\left(\alpha_{1jm}^{(2)}e^{i\tilde{k}_m^+D}-\beta_{1jm}^{(2)}\right)=e^{i\varphi/2}\frac{2}{W_N}\sum_l k_l^0S_{lm}\left(c_{1jl}u_0e^{-ik_l^+x_-}-d_{1jl}v_0e^{ik_l^+x_-}\right),\\
&\tilde{k}_m^0\left(\gamma_{1jm}^{(2)}-\delta_{1jm}^{(2)}e^{-i\tilde{k}_m^-D}\right)=e^{-i\varphi/2}\frac{2}{W_N}\sum_l k_l^0S_{lm}\left(c_{1jl}v_0e^{-ik_l^-x_-}-d_{1jl}u_0e^{ik_l^-x_-}\right),
\end{aligned} \tag{4.5}$$

where k_l^0 and $\tilde{k}_m^0$ are given by setting $E = 0$ in Eq. (4.2). Equations (4.3) and (4.5) are sufficient for determining the $4 \times (M_S + M_N)$ unknown coefficients. The scattering amplitude $a_{1jl}(\varphi, i\omega_n)$ is numerically calculated from these equations with $E \rightarrow i\omega_n$. Then the dc Josephson current is obtained via Eq. (2.8).

The critical current I_C is calculated at $T = 0.5$ and 1 K [Fig. 6(a)]. The dependence of I on φ is also shown in Fig. 6(b). We set $L = 100$ nm, $D = 20$ nm, $W_S = 120$ nm, and the values of the other parameters are the same as those in Sec. III. The length L of the normal region is about half of the coherence length. Thus, if one assumes that the mode conversion does not affect the total supercurrent flow, it is naturally expected that the $W_N - I_C$ curve shows a clear stepwise change from the discussion given in Sec. III. As expected, a stepwise change can be seen clearly in Fig. 6, which shows that the mode conversion is not relevant for the total magnitude of supercurrent.

Since the abrupt change of the width gives rise to normal reflections at $x = x_-$ and x_+, most electrons go and return many times in the narrow region until they reach one superconductor from the other. The interference caused by the multiple reflections influences not only the transmission probability of a single electron, i.e., the normal-state conductance, but also the Josephson current which is the flow of Cooper pairs. This is understood by the following consideration. The supercurrent is carried in the normal region by an electron and a hole which are Andreev reflected at S-Sm interfaces, creating or destructing a Cooper (Fig. 7). The electron and hole individually travel from one superconductor to the other superconductor while keeping their phase coherence. Since the Josephson effect is due to the phase-coherent propagation of Andreev-reflected electron and hole waves, the probability that each quasiparticle (electron or hole) goes through the constriction is a key factor determining the flow of supercurrent. Thus the multiple reflections at $x = x_-$ and x_+ give rise to resonances in the probability and, at the same time, in the critical current.

Some typical results on this geometrical interference effect are shown in Fig. 8. The length D of the nar-

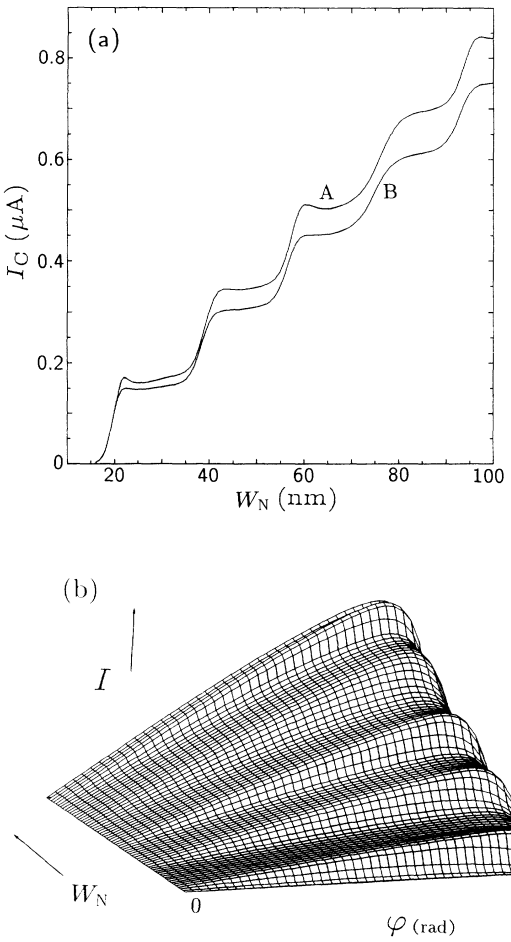

FIG. 6. (a) The critical current vs the width of the constriction at $T = 0.5$ K (A) and $T = 1$ K (B) and (b) the current vs the phase difference for various values of the width at $T = 0.5$ K.

row region is 50 nm, so the resonant structures are more evident than in Fig. 6. The dependence of I_C, curves (a) and (b), and of G, curve (c), on W_N is shown. The peaks are located in the same position in the three curves,

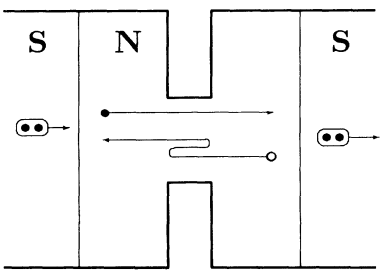

FIG. 7. Illustration of the supercurrent flow through the constriction. A Cooper pair travels from the left superconductor to the right, changing into a right-going electron and a left-going hole in the semiconductor. The hole is suffering normal reflections twice.

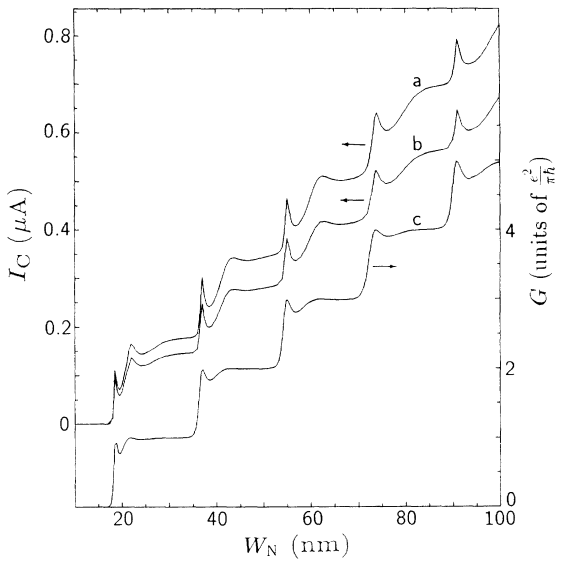

FIG. 8. The critical current (a) and (b), and the normal-state conductance (c), as a function of the width of the constriction. $D = 50$ nm, $L = 100$ nm (a) and 200 nm (b), and $T = 0.5$ K.

which confirms the above conjecture that the resonances are due to the interference of individual electrons. The resonances in the critical current come from the resonances in the transmission amplitude of electrons and holes through the constriction. This effect is very interesting in that the interference of individual electrons, which comes from the phase of a single-electron wave function, influences the Josephson effect, which has its origin in the phase of the condensate, i.e., Cooper pairs.

V. EFFECT OF NORMAL REFLECTION

So far we have assumed that the S-Sm interfaces are ideal ones. In actual samples, however, there is often a Schottky barrier at the interface, and the Fermi momentum is different between a superconductor and a semiconductor. Both give rise to normal reflections, in addition to the Andreev reflection, at the S-Sm interfaces: electron(-like)→electron(-like) and hole(-like)→hole(-like). In this section we examine the effect of the normal reflection on the dc Josephson effect.

We calculate the Josephson current in the adiabatic approximation, using the same model as in Sec. III. Following the treatment by Blonder *et al.*,[29] we incorporate the normal reflections phenomenologically by introducing a δ-function potential at the interfaces; the single-electron Hamiltonian is given by

$$H(x,y) = -\frac{\hbar^2}{2m}\left(\frac{\partial^2}{\partial x^2}+\frac{\partial^2}{\partial y^2}\right) + V\left[\delta(x)+\delta(x-L)\right] - E_F. \tag{5.1}$$

Following the same path as in Sec. III we have the matching equations at $x = 0$ and $x = L$:

$$u_0 + a_{1j}v_0 + b_{1j}u_0 = \alpha_{1j} + \beta_{1j}, \quad v_0 + a_{1j}u_0 + b_{1j}v_0 = \gamma_{1j} + \delta_{1j},$$

$$e^{i\varphi/2}(c_{1j}u_0 + d_{1j}v_0) = \alpha_{1j}\exp\left(i\int_0^L k_j^+(x)dx\right) + \beta_{1j}\exp\left(-i\int_0^L k_j^+(x)dx\right),$$

$$e^{-i\varphi/2}(c_{1j}v_0 + d_{1j}u_0) = \gamma_{1j}\exp\left(i\int_0^L k_j^-(x)dx\right) + \delta_{1j}\exp\left(-i\int_0^L k_j^-(x)dx\right),$$

$$\alpha_{1j} - \beta_{1j} - (u_0 + a_{1j}v_0 - b_{1j}u_0) = -2iZ_j(\alpha_{1j} + \beta_{1j}), \tag{5.2}$$

$$\gamma_{1j} - \delta_{1j} - (v_0 + a_{1j}u_0 - b_{1j}v_0) = -2iZ_j(\gamma_{1j} + \delta_{1j}),$$

$$e^{i\varphi/2}(c_{1j}u_0 - d_{1j}v_0) - \left[\alpha_{1j}\exp\left(i\int_0^L k_j^+(x)dx\right) - \beta_{1j}\exp\left(-i\int_0^L k_j^+(x)dx\right)\right] = -2iZ_j e^{i\varphi/2}(c_{1j}u_0 + d_{1j}v_0),$$

$$e^{-i\varphi/2}(c_{1j}v_0 - d_{1j}u_0) - \left[\gamma_{1j}\exp\left(i\int_0^L k_j^-(x)dx\right) - \delta_{1j}\exp\left(-i\int_0^L k_j^-(x)dx\right)\right] = -2iZ_j e^{-\varphi/2}(c_{1j}v_0 + d_{1j}u_0),$$

where $Z_j \equiv mV/\hbar^2 p_j$. From the solution of Eq. (5.2) we obtain the dc Josephson current as

$$I = \frac{2e\Delta_0^2}{\hbar\beta}\sum_{j=1}^{N}\sum_{\omega_n}\frac{\sin\varphi}{\Gamma}, \tag{5.3}$$

where

$$\begin{aligned}\Gamma = {} & [\omega_n^2 + \Omega_n^2 + 4Z_j^2(1+Z_j^2)\Omega_n^2]\cosh\tilde{\Phi}_j^- + 2\omega_n\Omega_n(1+2Z_j^2)\sinh\tilde{\Phi}_j^- + 4Z_j^2(1-Z_j^2)\Omega_n^2\cos\tilde{\Phi}_j^+ \\ & + 8Z_j^3\Omega_n^2\sin\tilde{\Phi}_j^+ + \Delta_0^2\cos\varphi, \\ \tilde{\Phi}_j^- = {} & \frac{1}{i}\int_0^L (k_j^+ - k_j^-)dx\Big|_{E\to i\omega_n}, \quad \tilde{\Phi}_j^+ = \int_0^L (k_j^+ + k_j^-)dx\Big|_{E\to i\omega_n}\end{aligned} \tag{5.4}$$

The wave number $k_j^{\pm}(x)$ has already been defined in Eq. (3.4) with $W(x)$ given by Eq. (3.11).

In Fig. 9 we show the critical current at $T = 0$ as a function of the minimum width W_N for various values of $Z \equiv mV/\hbar^2 p_0$, where $p_0 \equiv (2mE_F/\hbar^2)^{1/2}$. The value of W_S is chosen as 200 nm, and the other parameters are the same as in Sec. III. Figure 9 shows that I_C-W_N curve begins to show clear resonant peaks as the parameter Z increases, i.e., as the normal reflection becomes dominant. These peaks originate from the interference of quasiparticles which go and return many times in the semiconductor. This is easily seen by rewriting Eq. (5.4) as

$$\begin{aligned}\frac{2\Gamma}{(\Omega_n^2 + \omega_n^2 + 2Z_j^2\Omega_n^2)^2\exp(-\tilde{\Phi}_j^-)} = {} & \left(1 + \frac{\Omega_n - \omega_n + 2Z_j^2\Omega_n}{\Omega_n + \omega_n + 2Z_j^2\Omega_n}\exp\left(-\tilde{\Phi}_j^- + i\varphi\right)\right)\left(1 + \frac{\Omega_n - \omega_n + 2Z_j^2\Omega_n}{\Omega_n + \omega_n + 2Z_j^2\Omega_n}\exp\left(-\tilde{\Phi}_j^- - i\varphi\right)\right) \\ & + \frac{4Z_j^2\Omega_n^2}{(\Omega_n + \omega_n + 2Z_j^2\Omega_n)^2}\left[(1 - iZ_j)^2\exp\left(2i\int_0^L \tilde{k}_j^+ dx\right) + (1 + iZ_j)^2\exp\left(-2i\int_0^L \tilde{k}_j^- dx\right)\right. \\ & \left. - 2(1 + Z_j^2)\exp\left(-\tilde{\Phi}_j^-\right)\cos\varphi\right],\end{aligned} \tag{5.5}$$

where $\tilde{k}_j^{\pm} \equiv k_j^{\pm}(E \to i\omega_n)$. The terms proportional to $\exp\left(-\tilde{\Phi}_j^-\right)$ on the right-hand side (rhs) of Eq. (5.5) correspond to the process in which an electron experiences the Andreev reflection at both S-Sm interfaces while making a round trip; an electron is reflected as a hole at an S-Sm interface and then the hole is reflected as an electron at the other S-Sm interface. These terms cause no interference. The interference comes from the term proportional to $\exp\left(2i\int_0^L \tilde{k}_j^+ dx\right)\left[\exp\left(-2i\int_0^L \tilde{k}_j^- dx\right)\right]$ which represents the round trip of an electron (a hole) having suffered the normal reflection at the S-Sm interfaces. A resonant peak in Fig. 9 appears when the rhs of Eq. (5.5) takes a minimum value. It is interesting to note that the resonant tunneling for a large-Z value exactly corresponds to the resonant-tunneling Josephson effect studied by van Houten,[8] although we consider only the static Josephson effect.

Figure 9 suggests that, when the normal reflection at the S-Sm interfaces exists, the stepwise increase in the

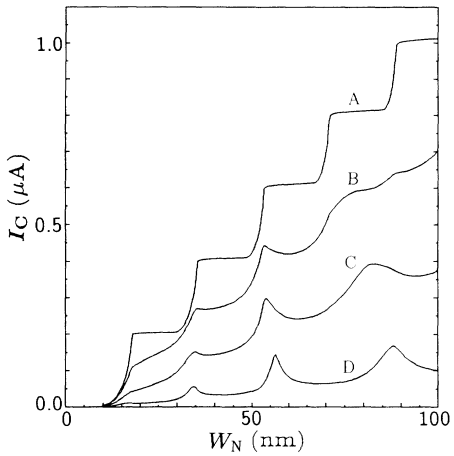

FIG. 9. The critical current as a function of the width at zero temperature. The normal reflection is incorporated into the theory via the parameter Z: $Z = 0$ (A), 0.2 (B), 0.5 (C), and 1.0 (D). We set $L = 100$ nm and $W_S = 200$ nm.

critical current can hardly be seen. Instead, resonant peaks are observed. In real systems, however, the finiteness of the phase coherence length L_ϕ and the intermode scattering discussed in Sec. IV may cut off the multiple reflections and make the resonant peaks broader. We shall consider an extreme case where only the direct (lowest order) process contributes to the Josephson current and the higher order processes involving multiply reflected quasiparticles are negligible. This is achieved by replacing the rhs of Eq. (5.5) by unity, and thus the Josephson current is given by

$$I = \frac{4e\Delta_0^2}{\hbar\beta} \sum_{j=1}^{N} \sum_{\omega_n} \frac{\sin\varphi}{(\Omega_n + \omega_n + 2Z_j^2\Omega_n)^2} \exp(-\tilde{\Phi}_j^-). \tag{5.5}$$

The I_C-W_N relation calculated from Eq. (5.5) is shown in Fig. 10. There is, of course, no resonant peak in the figure, but the critical current increases almost stepwise.

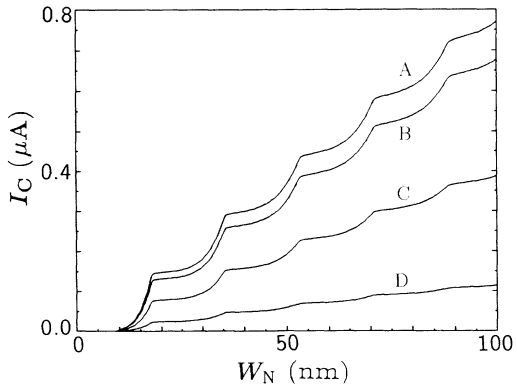

FIG. 10. The critical current calculated from Eq. (5.5). The parameters are the same as in Fig. 9.

The situation which could be achieved experimentally lies in between that shown in Fig. 9 and in Fig. 10.

VI. CONCLUSIONS

The dc Josephson effect of an SQPC has been investigated both in the adiabatic-transport regime and in the nonadiabatic-transport regime. The Josephson current is calculated from the scattering amplitude of the Andreev reflection which is obtained by solving the Bogoliubov-de Gennes equation. It is shown that, for the ideal S-Sm interface, the critical current increases stepwise as a function of the constriction width. The step height depends not only on the superconducting gap Δ_0 but also on the separation between two superconductors L; the geometry of the system also influences the critical current. Using an artificial model in which the width changes suddenly from W_S to W_N and vice versa, it has also been shown that resonant peaks appear which are due to the interference of an individual quasiparticle which goes and returns in the narrow region many times.

The Schottky barrier and the mismatch of the Fermi momentum cause the normal reflection at the S-Sm interface and may prevent the observation of the stepwise increase, i.e., *quasiquantization* of the critical current. This issue has also been studied phenomenologically. Our findings are the following. If all the higher-order processes involving multiple normal reflections contribute equally to the supercurrent, then the I_C-W_N curve shows resonances corresponding to the resonant tunneling of Cooper pairs through a resonant level formed in the semiconductor by the diagonal potential barrier rather than by the off-diagonal (pair) potential. On the other hand, if the multiple normal reflection is not effective, the resonances disappear and the stepwise change can be seen. Although experiments for confirming our idea may be difficult, it is expected that in the near future when a high-mobility SQPC with clean S-Sm interfaces is fabricated, the *quasiquantization* of the critical current or alternatively the resonant structures due to the normal reflection will be observed experimentally.

ACKNOWLEDGMENTS

This work was supported in part by a Grant-in-Aid from the Ministry of Education, Science, and Culture of Japan, and numerical calculations were performed on HITAC S-820 at the computer center of the University of Tokyo.

APPENDIX

In this appendix we describe the method to construct the retarded Green's function from the solutions of the BdG equation.

The wave functions are plane waves in the regions $x < 0$ and $x > L$ since the pair potential is constant. In addition to the wave function given in Eqs. (2.4) and (2.5), there are three other types of wave functions.[15] The wave function for the process in which a holelike quasiparticle is injected from the left is written as

$$\psi_{2j}(x,y)=\begin{cases} e^{-ip_j^- x}\sqrt{\frac{2}{W_S}}\sin[q_j(y+W_S/2)]\begin{pmatrix}v_0\\u_0\end{pmatrix} \\ \quad+\sqrt{\frac{2}{W_S}}\sum_{k=1}^{\infty}\left[a_{2jk}e^{-ip_k^+ x}\begin{pmatrix}u_0\\v_0\end{pmatrix}+b_{2jk}e^{ip_k^- x}\begin{pmatrix}v_0\\u_0\end{pmatrix}\right]\sin[q_k(y+W_S/2)], & x<0 \\ \sqrt{\frac{2}{W_S}}\sum_{k=1}^{\infty}\left[c_{2jk}e^{-ip_k^- x}\begin{pmatrix}v_0e^{i\varphi/2}\\u_0e^{-i\varphi/2}\end{pmatrix}+d_{2jk}e^{ip_k^+ x}\begin{pmatrix}u_0e^{i\varphi/2}\\v_0e^{-i\varphi/2}\end{pmatrix}\right]\sin[q_k(y+W_S/2)], & x>L. \end{cases} \tag{A1}$$

The other two types of wave functions representing the process in which an electronlike, or a holelike quasiparticle is injected from the right are written, respectively, as

$$\psi_{3j}(x,y)=\begin{cases} \sqrt{\frac{2}{W_S}}\sum_{k=1}^{\infty}\left[c_{3jk}e^{-ip_k^+ x}\begin{pmatrix}u_0\\v_0\end{pmatrix}+d_{3jk}e^{ip_k^- x}\begin{pmatrix}v_0\\u_0\end{pmatrix}\right]\sin[q_k(y+W_S/2)], & x<0 \\ e^{-ip_j^+ x}\sqrt{\frac{2}{W_S}}\sin[q_j(y+W_S/2)]\begin{pmatrix}u_0e^{i\varphi/2}\\v_0e^{-i\varphi/2}\end{pmatrix} \\ \quad+\sqrt{\frac{2}{W_S}}\sum_{k=1}^{\infty}\left[a_{3jk}e^{-ip_k^- x}\begin{pmatrix}v_0e^{i\varphi/2}\\u_0e^{-i\varphi/2}\end{pmatrix}+b_{3jk}e^{ip_k^+ x}\begin{pmatrix}u_0e^{i\varphi/2}\\v_0e^{-i\varphi/2}\end{pmatrix}\right]\sin[q_k(y+W_S/2)], & x>L, \end{cases} \tag{A2}$$

and

$$\psi_{4j}(x,y)=\begin{cases} \sqrt{\frac{2}{W_S}}\sum_{k=1}^{\infty}\left[c_{4jk}e^{ip_k^- x}\begin{pmatrix}v_0\\u_0\end{pmatrix}+d_{4jk}e^{-ip_k^+ x}\begin{pmatrix}u_0\\v_0\end{pmatrix}\right]\sin[q_k(y+W_S/2)], & x<0 \\ e^{ip_j^- x}\sqrt{\frac{2}{W_S}}\sin[q_j(y+W_S/2)]\begin{pmatrix}v_0e^{i\varphi/2}\\u_0e^{-i\varphi/2}\end{pmatrix} \\ \quad+\sqrt{\frac{2}{W_S}}\sum_{k=1}^{\infty}\left[a_{4jk}e^{ip_k^+ x}\begin{pmatrix}u_0e^{i\varphi/2}\\v_0e^{-i\varphi/2}\end{pmatrix}+b_{4jk}e^{-ip_k^- x}\begin{pmatrix}v_0e^{i\varphi/2}\\u_0e^{-i\varphi/2}\end{pmatrix}\right]\sin[q_k(y+W_S/2)], & x>L. \end{cases} \tag{A3}$$

It is easily verified that the coefficients $a_{ijk}(E,\varphi)$, $b_{ijk}(E,\varphi)$, $c_{ijk}(E,\varphi)$, and $d_{ijk}(E,\varphi)$ satisfy the following detailed balance relations:

$$\begin{aligned} &p_k^- a_{1jk}(\varphi)=p_j^+ a_{2kj}(-\varphi), \quad p_k^- a_{3jk}(\varphi)=p_j^+ a_{4kj}(-\varphi), \\ &p_k^+ b_{1jk}(\varphi)=p_j^+ b_{1kj}(-\varphi), \quad p_k^- b_{2jk}(\varphi)=p_j^- b_{2kj}(-\varphi), \\ &p_k^+ b_{3jk}(\varphi)=p_j^+ b_{3kj}(-\varphi), \quad p_k^- b_{4jk}(\varphi)=p_j^- b_{4kj}(-\varphi), \\ &p_k^+ c_{1jk}(\varphi)=p_j^+ c_{3kj}(-\varphi), \quad p_k^- c_{2jk}(\varphi)=p_j^- c_{4kj}(-\varphi), \\ &p_k^- d_{1jk}(\varphi)=p_j^+ d_{4kj}(-\varphi), \quad p_k^+ d_{2jk}(\varphi)=p_j^- d_{3kj}(-\varphi). \end{aligned} \tag{A4}$$

From these relations, it is proved that the retarded Green's function $G^r(x,y:x',y';E)$ is given by

$$G^r(x,y:x',y';E)=\begin{cases} \sum_{j,k=1}^{\infty}[\alpha_{1jk}\psi_{3j}(x,y)\tilde{\psi}_{1k}^{\mathbf{t}}(x',y')+\alpha_{2jk}\psi_{3j}(x,y)\tilde{\psi}_{2k}^{\mathbf{t}}(x',y') \\ \qquad+\alpha_{3jk}\psi_{4j}(x,y)\tilde{\psi}_{1k}^{\mathbf{t}}(x',y')+\alpha_{4jk}\psi_{4j}(x,y)\tilde{\psi}_{2k}^{\mathbf{t}}(x',y')], & x\le x' \\ \sum_{j,k=1}^{\infty}[\beta_{1jk}\psi_{1j}(x,y)\tilde{\psi}_{3k}^{\mathbf{t}}(x',y')+\beta_{2jk}\psi_{2j}(x,y)\tilde{\psi}_{3k}^{\mathbf{t}}(x',y') \\ \qquad+\beta_{3jk}\psi_{1j}(x,y)\tilde{\psi}_{4k}^{\mathbf{t}}(x',y')+\beta_{4jk}\psi_{2j}(x,y)\tilde{\psi}_{4k}^{\mathbf{t}}(x',y')], & x\ge x', \end{cases} \tag{A5}$$

where $\tilde{f}(\varphi)\equiv f(-\varphi)$, $\tilde{\psi}_{ij}^{\mathbf{t}}$ is the transposition of $\tilde{\psi}_{ij}$, and α_i and β_i are the solutions of the following equations:

$$\sum_{l=1}^{\infty}(\alpha_{1jl}c_{3lk}+\alpha_{3jl}d_{4lk})=-\frac{imE}{\hbar^2 p_j^+\Omega}\delta_{j,k},\quad \sum_{l=1}^{\infty}(\alpha_{2jl}c_{3lk}+\alpha_{4jl}d_{4lk})=0,$$
$$\sum_{l=1}^{\infty}(\alpha_{1jl}d_{3lk}+\alpha_{3jl}c_{4lk})=0,\quad \sum_{l=1}^{\infty}(\alpha_{2jl}d_{3lk}+\alpha_{4jl}c_{4lk})=-\frac{imE}{\hbar^2 p_j^-\Omega}\delta_{j,k},$$
$$\sum_{l=1}^{\infty}(\beta_{1jl}\tilde{c}_{3lk}+\beta_{3jl}\tilde{d}_{4lk})=-\frac{imE}{\hbar^2 p_j^+\Omega}\delta_{j,k},\quad \sum_{l=1}^{\infty}(\beta_{1jl}\tilde{d}_{3lk}+\beta_{3jl}\tilde{c}_{4lk})=0,$$
$$\sum_{l=1}^{\infty}(\beta_{2jl}\tilde{c}_{3lk}+\beta_{4jl}\tilde{d}_{4lk})=0,\quad \sum_{l=1}^{\infty}(\beta_{2jl}\tilde{d}_{3lk}+\beta_{4jl}\tilde{c}_{4lk})=-\frac{imE}{\hbar^2 p_j^-\Omega}\delta_{j,k}. \tag{A6}$$

Substituting these equations into Eq. (A5) yields, for $x,x'\le 0$,

$$\begin{aligned}G^r(x,y:x',y';E)=&-\frac{2imE}{\hbar^2\Omega W_S}\sum_{j=1}^{\infty}\frac{1}{p_j^+}\sin[q_j(y'+W_S/2)]\\
&\times\Bigg[\Bigg(e^{ip_j^+|x-x'|}\sin[q_j(y+W_S/2)]\\
&\quad+\sum_{k=1}^{\infty}b_{1jk}e^{-i(p_k^+x+p_j^+x')}\sin[q_k(y+W_S/2)]\Bigg)\begin{pmatrix}u_0^2 & u_0v_0\\ u_0v_0 & v_0^2\end{pmatrix}\\
&\quad+\sum_{k=1}^{\infty}a_{1jk}e^{i(p_k^-x-p_j^+x')}\sin[q_k(y+W_S/2)]\begin{pmatrix}u_0v_0 & v_0^2\\ u_0^2 & u_0v_0\end{pmatrix}\Bigg]\\
&-\frac{2imE}{\hbar^2\Omega W_S}\sum_{j=1}^{\infty}\frac{1}{p_j^-}\sin[q_j(y'+W_S/2)]\\
&\times\Bigg[\Bigg(e^{-ip_j^-|x-x'|}\sin[q_j(y+W_S/2)]\\
&\quad+\sum_{k=1}^{\infty}b_{2jk}e^{i(p_k^-x+p_j^-x')}\sin[q_k(y+W_S/2)]\Bigg)\begin{pmatrix}v_0^2 & u_0v_0\\ u_0v_0 & u_0^2\end{pmatrix}\\
&\quad+\sum_{k=1}^{\infty}a_{2jk}e^{-i(p_k^+x-p_j^-x')}\sin[q_k(y+W_S/2)]\begin{pmatrix}u_0v_0 & u_0^2\\ v_0^2 & u_0v_0\end{pmatrix}\Bigg].\end{aligned} \tag{A7}$$

[1] B. J. van Wees, H. van Houten, C. W. J. Beenakker, J. G. Williamson, L. P. Kouwenhoven, D. van der Marel, and C. T. Foxon, Phys. Rev. Lett. **60**, 848 (1988).

[2] D. A. Wharam, T. J. Thornton, R. Newbury, M. Pepper, H. Ahmed, J. E. F. Frost, D. G. Hasko, D. C. Peacock, D. A. Ritchie, and G. A. C. Jones, J. Phys. C **21**, L209 (1988).

[3] C. W. J. Beenakker and H. van Houten, in *Solid State Physics*, edited by H. Ehrenreich and D. Turnbull (Academic, New York, 1991), Vol. 44, p. 1.

[4] H. Takayanagi and T. Kawakami, Phys. Rev. Lett. **54**, 2449 (1985).

[5] I. O. Kulik and A. N. Omel'yanchuk, Fiz. Nizk. Temp. **4**, 296 (1978) [Sov. J. Low Temp. Phys. **4**, 142 (1978)].

[6] At finite temperature near the critical temperature, another length scale, $\xi_N=\hbar v_F/\pi k_B T$, supersedes ξ.

[7] C. W. J. Beenakker and H. van Houten, Phys. Rev. Lett. **66**, 3056 (1991).

[8] H. van Houten, Appl. Phys. Lett. **58**, 1326 (1991).

[9] A. Furusaki, H. Takayanagi, and M. Tsukada, Phys. Rev. Lett. **67**, 132 (1991).

[10] C. W. J. Beenakker and H. van Houten, in *Proceedings of the International Symposium on Nanostructures and Mesoscopic Systems, Santa Fe;* in *SQUID'91*, edited by H. Koch and H. Lübbig (Springer-Verlag, to be published).

[11] B. J. van Wees, K.-M. H. Lenssen, and C. J. P. M. Harmans, Phys. Rev. B **44**, 470 (1991).

[12] A. Furusaki, H. Takayanagi, and M. Tsukada, in *SQUID'91* (Ref. 10).

[13] P. G. de Gennes, *Superconductivity of Metals and Alloys* (Benjamin, New York, 1966).

[14] A. F. Andreev, Zh. Eksp. Teor. Fiz. **46**, 1823 (1964) [Sov. Phys. JETP **19**, 1228 (1964)].

[15] The method is explained for a one-dimensional model by A. Furusaki and M. Tsukada, Solid State Commun. **78**, 299 (1991).

[16] Y. Tanaka and M. Tsukada, Phys. Rev. B **42**, 2066 (1990).

[17] M. Ashida, S. Aoyama, J. Hara, and K. Nagai, Phys. Rev. B **40**, 8673 (1989); M. Ashida, J. Hara, and K. Nagai, Phys. Rev. B **45**, 828 (1992).

[18] A. P. van Gelder, Phys. Rev. **181**, 787 (1969).

[19] I. O. Kulik, Zh. Eksp. Teor. Fiz. **57**, 1745 (1969) [Sov. Phys. JETP **30**, 944 (1970)].

[20] C. Ishii, Prog. Theor. Phys. **44**, 1525 (1970); **47**, 1464

(1972).
[21] J. Bardeen and J. L. Johnson, Phys. Rev. B **5**, 72 (1972).
[22] A. V. Svidzinsky, T. N. Antsygina, and E. N. Bratus', J. Low Temp. Phys. **10**, 131 (1973).
[23] M. Büttiker and T. M. Klapwijk, Phys. Rev. B **33**, 5114 (1986).
[24] A. Furusaki and M. Tsukada, Phys. Rev. B **43**, 10 164 (1991).
[25] H. Plehn, U. Gunsenheimer, and R. Kümmel, J. Low Temp. Phys. **83**, 71 (1991).
[26] In this paper we apply the simplest WKB approximation, which is sufficient for our qualitative discussion in the adiabatic transport. For a more complete discussion of the WKB method, see J. Bardeen, R. Kümmel, A. E. Jacobs, and L. Tewordt, Phys. Rev. **187**, 556 (1969) and Ref. 10.
[27] The critical current calculated in Eq. (5) of Ref. 9 is wrong by a numerical factor, $2/\pi$.
[28] The values of N and m we adopt are typical ones for p-type InAs.
[29] G. E. Blonder, M. Tinkham, and T. M. Klapwijk, Phys. Rev. B **25**, 4515 (1982).